Entropy **2009**, *11*, 513 - 528; doi:10.3390/e11030513

OPEN ACCESS

entropy

ISSN 1099-4300

www.mdpi.com/journal/entropy

Article

Scale-Based Gaussian Coverings: Combining Intra and Inter Mixture Models in Image Segmentation

Fionn Murtagh [1,2,⋆], Pedro Contreras [2] and Jean-Luc Starck [3,4]

[1] Science Foundation Ireland, Wilton Park House, Wilton Place, Dublin 2, Ireland

[2] Department of Computer Science, Royal Holloway University of London, Egham TW20 0EX, UK; E-Mail: pedro@cs.rhul.ac.uk

[3] CEA-Saclay, DAPNIA/SEDI-SAP, Service d'Astrophysique, 91191 Gif sur Yvette, France; E-Mail: jstarck@cea.fr

[4] Laboratoire AIM (UMR 7158), CEA/DSM-CNRS, Université Paris Diderot, Diderot, IRFU, SEDI-SAP, Service d'Astrophysique, Centre de Saclay, F-91191 Gif-Sur-Yvette cedex, France

[⋆] Author to whom correspondence should be addressed: E-Mail: fmurtagh@acm.org; Tel.: +44 1784 443429; Fax: +44 1784 439786.

Received: 1 September 2009 / Accepted: 14 September 2009 / Published: 24 September 2009

Abstract: By a "covering" we mean a Gaussian mixture model fit to observed data. Approximations of the Bayes factor can be availed of to judge model fit to the data within a given Gaussian mixture model. Between families of Gaussian mixture models, we propose the Rényi quadratic entropy as an excellent and tractable model comparison framework. We exemplify this using the segmentation of an MRI image volume, based (1) on a direct Gaussian mixture model applied to the marginal distribution function, and (2) Gaussian model fit through k-means applied to the 4D multivalued image volume furnished by the wavelet transform. Visual preference for one model over another is not immediate. The Rényi quadratic entropy allows us to show clearly that one of these modelings is superior to the other.

Keywords: image segmentation; clustering; model selection; minimum description length; Bayes factor; Rényi entropy; Shannon entropy

---

1. Introduction

We begin with some terminology used. Segments are contiguous clusters. In an imaging context, this means that clusters contain adjacent or contiguous pixels. For typical 2D (two-dimensional) images, we may also consider the 1D (one-dimensional) marginal which provides an empirical estimate of the pixel (probability) density function or PDF. For 3D (three-dimensional) images, we can consider 2D marginals, based on the voxels that constitute the 3D image volume, or also a 1D overall marginal. An image is representative of a signal. More loosely a signal is just data, mostly here with neccessary sequence or adjacency relationships. Often we will use interchangeably the terms image, image volume if relevant, signal and data.

The word "model" is used, in general, in many senses–statistical [1], mathematical, physical models; mixture model; linear model; noise model; neural network model; sparse decomposition model; even, in different senses, data model. In practice, firstly and foremostly for algorithmic tractability, models of whatever persuasion tend to be homogeneous. In this article we wish to broaden the homogeneous mixture model framework in order to accommodate heterogeneity at least as relates to resolution scale. Our motivation is to have a rigorous model-based approach to data clustering or segmentation, that also and in addition encompasses resolution scale.

Figure 1. Clusters of all morphologies are sought. Figure courtesy of George Djorgovski, Caltech.

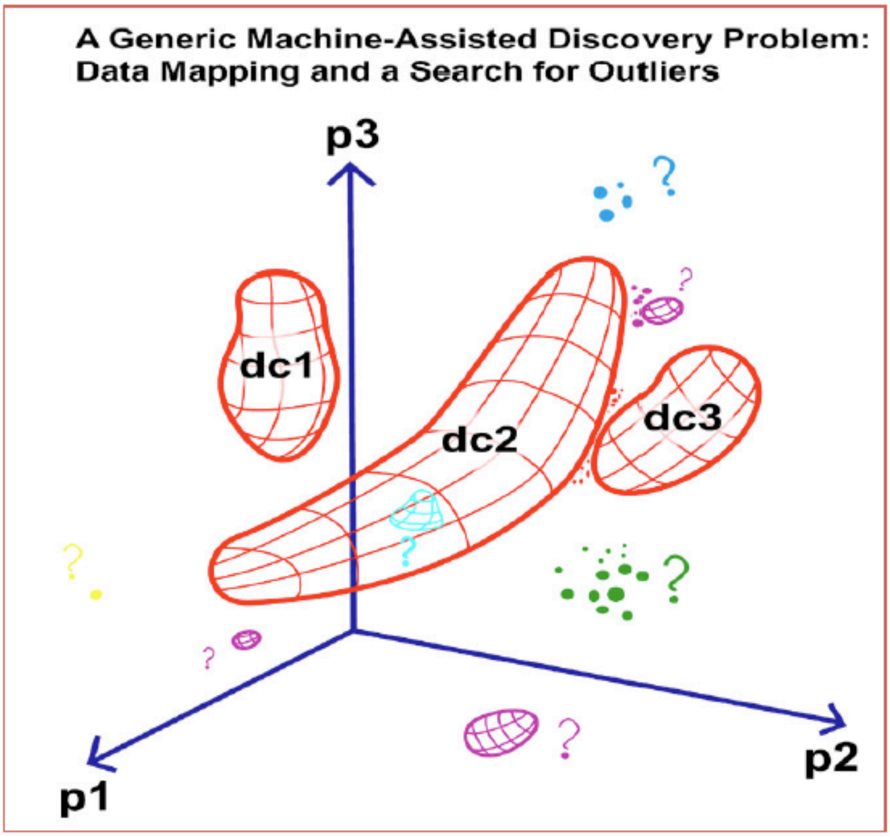

In Figure 1 [2], the clustering task is portrayed in its full generality. One way to address it is to build up parametrized clusters, for example using a Gaussian mixture model (GMM), so that the cluster "pods" are approximated by the mixture made up of the cluster component "peas" (a viewpoint expressed by A.E. Raftery, quoted in [3]).

A step beyond a pure "peas" in a "pod" approach to clustering is a hierarchical approach. Application specialists often consider hierarchical algorithms as more versatile than their partitional counterparts (for example, k-means or Gaussian mixture models) since the latter tend to work well only on data sets having isotropic clusters [4]. So in [5], we segmented astronomical images of different observing filters, that had first been matched such that they related to exactly the same fields of view and pixel resolution. For the segmentation we used a Markov random field and Gaussian mixture model; followed by a within-segment GMM clustering on the marginals. Further within-cluster marginal clustering could be continued if desired. For model fit, we used approximations of the Bayes factor: the pseudo-likelihood information criterion to start with, and for the marginal GMM work, a Bayesian information criterion. This hierarchical- or tree-based approach is rigorous and we do not need to go beyond the Bayes factor model evaluation framework. The choice of segmentation methods used was due to the desire to use contiguity or adjacency information whenever possible, and when not possible to fall back on use of the marginal. This mixture of segmentation models is a first example of what we want to appraise in this work.

What now if we cannot (or cannot conveniently) match the images beforehand? In that case, segments or clusters in one image will not necessarily correspond to corresponding pixels in another image. That is a second example of where we want to evaluate different families of models.

A third example of what we want to cater for in this work is the use of wavelet transforms to substitute for spatial modeling (e.g., Markov random field modeling). In this work one point of departure is a Gaussian mixture model (GMM) with model selection using the Bayes information criterion (BIC) approximation to the Bayes factor. We extend this to a new hierarchical context. We use GMMs on resolution scales of a wavelet transform. The latter is used to provide resolution scale. Between resolution scales we do not seek a strict subset or embedding relationship over fitted Gaussians, but instead accept a lattice relation. We focus in particular on the global quality of fit of this wavelet-transform based Gaussian modeling. We show that a suitable criterion of goodness of fit for cross-model family evaluations is given by Rényi quadratic entropy.

1.1. Outline of the Article

In Section 2 we review briefly how modeling, with Gaussian mixture modeling in mind, is mapped into information.

In Section 3 we motivate Gaussian mixture modeling as a general clustering approach.

In Section 4 we introduce entropy and focus on the additivity property. This property is importatant to us in the following context. Since hierarchical cluster modeling, not well addressed or supported by Gaussian mixture modeling, is of practical importance we will seek to operationalize a wavelet transform approach to segmentation. The use of entropy in this context is discussed in Section 5.

The fundamental role of Shannon entropy together with some other definitions of entropy in signal and noise modeling is reviewed in Section 6. Signal and noise modeling are potentially usable for image segmentation.

For the role of entropy in image segmentation, section 2 presented the state of the art relative to Gaussian mixture modeling; and Section 6 presented the state of the art relative to (segmentation-relevant) filtering.

What if we have segmentations obtained through different modelings? Section 7 addresses this through the use of Rényi quadratic entropy. Finally, Section 8 presents a case study.

2. Minimum Description Length and Bayes Information Criterion

For what we may term a homogenous modeling framework, the minimum description length, MDL, associated with Shannon entropy [6], will serve us well. However as we will now describe it does not cater for hierarchically embedded segments or clusters. An example of where hierarchical embedding, or nested clusters, come into play can be found in [5].

Following Hansen and Yu [7], we consider a model class, Θ, and an instantiation of this involving parameters θ to be estimated, yielding $\hat{\theta}$. We have $\theta \in \mathbb{R}^k$ so the parameter space is k-dimensional. Our observation vectors, of dimension m, and of cardinality n, are defined as: $X = \{x_i | 1 \leq i \leq n\}$. A model, M, is defined as $f(X|\theta), \theta \in \Theta \subset \mathbb{R}^k, X = \{x_i | 1 \leq i \leq n\}, x_i \in \mathbb{R}^m, X \subset \mathbb{R}^m$. The maximum likelihood estimator (MLE) of θ is $\hat{\theta}$: $\hat{\theta} = \text{argmax}_\theta f(X|\theta)$.

Using Shannon information, the description length of X based on a set of parameter values θ is: $-\log f(X|\theta)$. We need to transmit parameters also (as, for example, in vector quantization). So overall code length is: $-\log f(X|\theta) + L(\theta)$. If the number of parameters is always the same, then $L(\theta)$ can be constant. Minimizing $-\log f(X|\theta)$ over θ is the same as maximizing $f(X|\theta)$, so if $L(\theta)$ is constant, then MDL (minimum description length) is identical to maximum likelihood, ML.

The MDL information content of the ML, or equally Bayesian maximum a posteriori (MAP) estimate, is the code length of $-\log f(X|\hat{\theta}) + L(\hat{\theta})$. First, we need to encode the k coordinates of $\hat{\theta}$, where k is the (Euclidean) dimension of the parameter space. Using the uniform encoder for each dimension, the precision of coding is then $1/\sqrt{n}$ implying that the magnitude of the estimation error is $1/\sqrt{n}$. So the price to be paid for communicating $\hat{\theta}$ is $k \cdot (-\log 1/\sqrt{n}) = \frac{k}{2} \log n$ nats [7]. Going beyond the uniform coder is also possible with the same outcome.

In summary, MDL with simple suppositions here (in other circumstances we could require more than two stages, and consider other coders) is the sum of code lengths for (i) encoding data using a given model; and (ii) transmitting the choice of model. The outcome is minimal $-\log f(X|\hat{\theta}) + \frac{k}{2} \log n$.

In the Bayesian approach we assign a prior to each model class, and then we use the overall posterior to select the best model. Schwarz's Bayesian Information Criterion (BIC), which approximates the Bayes factor of posterior ratios, takes the form of the same penalized likelihood, $-\log f(X|\hat{\theta}) + \frac{k}{2} \log n$, where $\hat{\theta}$ = ML or MAP estimate of θ. See [8] for case studies using BIC.

3. Segmentation of Arbitrary Signal through a Gaussian Mixture Model

Notwithstanding the fact that often signal is not Gaussian, cf. the illustration of Figure 1, we can fit observational data–density f with support in m-dimensional real space, $\mathbb{R}^m$ – by Gaussians. Consider the case of heavy tailed distributions.

Heavy tailed probability distributions, examples of which include long memory or $1/f$ processes (appropriate for financial time series, telecommunications traffic flows, etc.) can be modeled as a generalized Gaussian distribution (GGD, also known as power exponential, α-Gaussian distribution, or generalized Laplacian distribution):

$$f(x) = \frac{\beta}{2\alpha\Gamma(1/\beta)} \exp -(\mid x \mid /\alpha)^{\beta}$$

where

– scale parameter, α, represents the standard deviation,
– the gamma function, $\Gamma(a) = \int_0^\infty x^{a-1} e^{-x} dx$, and
– shape parameter, β, is the rate of exponential decay, $\beta > 0$.

A value of $\beta = 2$ gives us a Gaussian distribution. A value of $\beta = 1$ gives a double exponential or Laplace distribution. For $0 < \beta < 2$, the distribution is heavy tailed. For $\beta > 2$, the distribution is light tailed.

Heavy tailed noise can be modeled by a Gaussian mixture model with enough terms [9]. Similarly, in speech and audio processing, low-probability and large-valued noise events can be modeled as Gaussian components in the tail of the distribution. A fit of this fat tail distribution by a Gaussian mixture model is commonly carried out [10]. As in Wang and Zhao [10], one can allow Gaussian component PDFs to recombine to provide the clusters which are sought. These authors also found that using priors with heavy tails, rather than using standard Gaussian priors, gave more robust results. But the benefit appears to be very small.

Gaussian mixture modeling of heavy tailed noise distributions, e.g. genuine signal and flicker or pink noise constituting a heavy tail in the density, is therefore feasible. A solution is provided by a weighted sum of Gaussian densities often with decreasing weights corresponding to increasing variances. Mixing proportions for small (tight) variance components are large (e.g., 0.15 to 0.3) whereas very large variance components have small mixing proportions.

Figures 2 and 3 illustrate long-tailed behavior and show how marginal density Gaussian model fitting works in practice. The ordinates give frequencies. See further discussion in [11, 12].

4. Additive Entropy

Background on entropy can be found e.g., in [13]. Following Hartley's 1928 treatment of equiprobable events, Shannon in 1948 developed his theory around expectation. In 1960 Rényi developed a recursive rather than linear estimation. Various other forms of entropy are discussed in [14].

Consider density f with support in $\mathbb{R}^m$. Then:

- Shannon entropy: $H_S = -\int f(x) \log f(x) dx$
- Rényi entropy: $H_{R\alpha} = \frac{1}{1-\alpha} \log \int f(x)^\alpha dx$ for $\alpha > 0, \alpha \neq 1$.

We have: $\lim_{\alpha \longrightarrow 1} H_{R\alpha} = H_S$. So $H_{R1} = H_S$. We also have: $H_{R\beta} \geq H_S \geq H_{R\gamma}$ for $0 < \beta < 1$ and $1 < \gamma$ (see e.g., [15], section 3.3). When $\alpha = 2$, H_{R2} is quadratic entropy.

Figure 2. Upper left: long-tailed histogram of marginal density of product of wavelet scales 4 and 5 of a 512×512 Lena image. Upper right, lower left, and lower right: histograms of classes 1, 2 and 3. These panels exemplify a nested model.

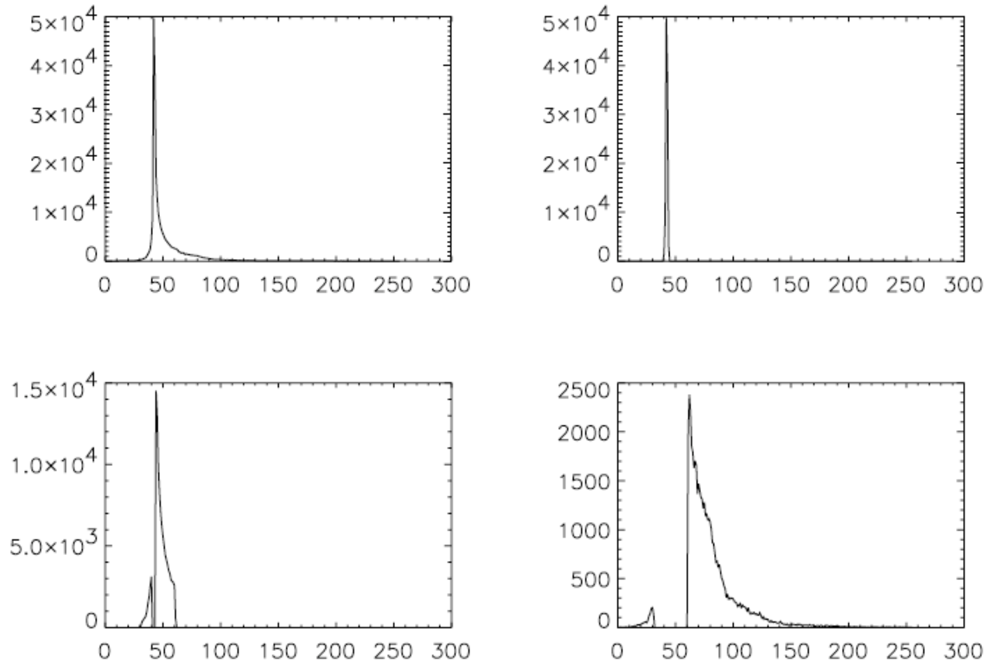

Both Shannon and Rényi quadratic entropy are additive, a property which will be availed of by us below for example when we we define entropy for a linear transform, i.e., an additive, invertible decomposition.

To show this, let us consider a system decomposed into independent events, A, B.

So $p(AB)$ (alternatively written: $p(A\&B)$ or $p(A + B)) = p(A)p(B)$. Shannon information is then $I_S^{AB} = -\log p(AB) = -\log p(A) - \log p(B)$, so the information of independent events is additive. Multiplying across by $p(AB)$, and taking $p(AB) = p(A)$ when considering only event A and similarly for B, leads to additivity of Shannon entropy for independent events, $H_S^{AB} = H_S^A + H_S^B$.

Similarly for Rényi quadratic entropy we use $p(AB) = p(A)p(B)$ and we have: $-\log p^2(AB) = -2\log p(AB) = -2\log (p(A)p(B)) = -2\log p(A) - 2\log p(B) = -\log p^2(A) - \log p^2(B)$.

5. The Entropy of a Wavelet Transformed Signal

The wavelet transform is a resolution-based decomposition–hence with an in-built spatial model: see e.g., [16, 17].

A redundant wavelet transform is most appropriate, even if decimated alternatives can be considered straightforwardly too. This is because segmentation, taking information into account at all available resolution scales, simply needs all available information. A non-redundant (decimated, e.g., pyramidal) wavelet transform is most appropriate for compression objectives, but it can destroy through aliasing potentially important faint features.

Figure 3. Overplotting of the histograms presented in Figure 2. This shows how the classes reconstitute the original data. The histogram of the latter is the upper left one in Figure 2.

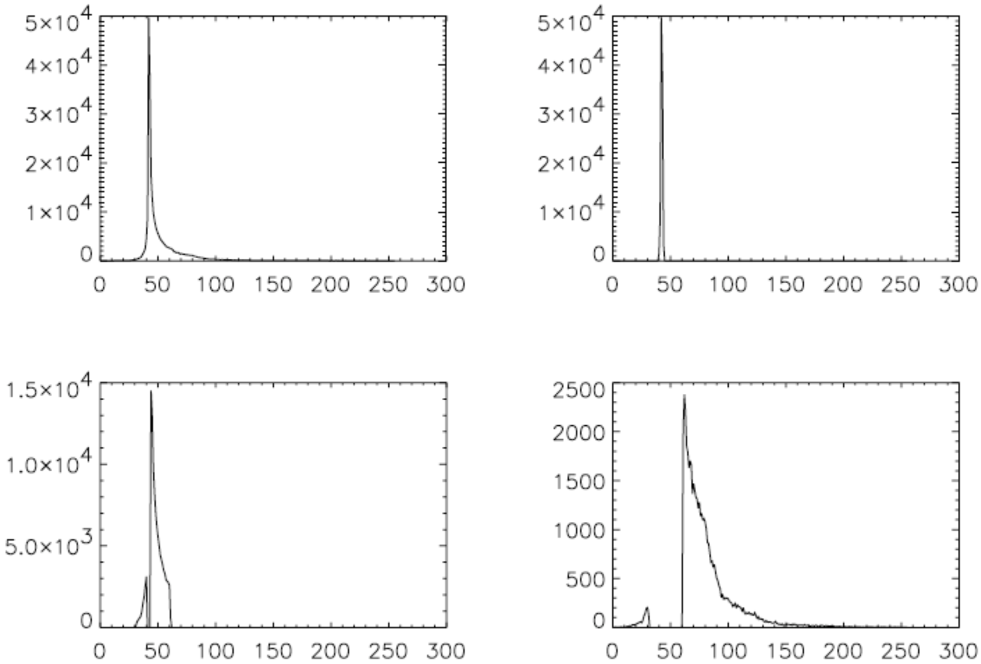

If f is the original signal, or images, then the following family of redundant wavelet transforms includes various discrete transforms such as the isotropic, B_3 spline, à trous transform, called the starlet wavelet transform in [17].

$$f = \sum_{s=1}^{S} w_s + w_{S+1} \tag{1}$$

where: w_{S+1} is the smooth continuum, not therefore wavelet coefficients; w_s are wavelet coefficients at scale s. Dimensions of f, w_s, w_{S+1} are all identical.

Nothing prevents us having a redundant Haar or, mutatis mutandis, redundant biorthogonal 9/7 wavelet transform (used in the JPEG-2000 compression standard). As mentined above, our choice of starlet transform is due to no damage being done, through decimation, to faint features in the image. As a matched filter the starlet wavelet function is appropriate for many types of biological, astronomical and other images [17].

Define the entropy, H, of the wavelet transformed signal as the sum of the entropies H^s at the wavelet resolution levels, s:

$$H = \sum_{s=1}^{S} H^s \tag{2}$$

Shannon and quadratic Rényi entropies are additive, as noted in section 4. For additivity, independence of the summed components is required. A redundant transform does not guarantee independence of resolution scales, $s = 1, 2, \ldots, S$. However in practice we usually have approximate independence. Our argument in favor of bypassing indepence of resolution scales is based on the practical and interpretation-related benefits of doing so.

Next we will review the Shannon entropy used in this context. Then we will introduce a new application of the Rényi quadratic entropy, again in this wavelet transform context.

6. Entropy Based on a Wavelet Transform and a Noise Model

Image filtering allows, as a special case, thresholding and reading off segmented regions. Such approaches have been used for very fast – indeed one could say with justice, turbo-charged–clustering. See [18, 19].

Noise models are particularly important in the physical sciences (cf. CCD, charge-coupled device, detectors) and the following approach was developed in [20]. Observed data f in the physical sciences are generally corrupted by noise, which is often additive and which follows in many cases a Gaussian distribution, a Poisson distribution, or a combination of both. Other noise models may also be considered. Using Bayes' theorem to evaluate the probability distribution of the realization of the original signal g, knowing the data f, we have:

$$\mathrm{p}(g|f) = \frac{\mathrm{p}(f|g).\mathrm{p}(g)}{\mathrm{p}(f)} \tag{3}$$

$\mathrm{p}(f|g)$ is the conditional probability distribution of getting the data f given an original signal g, i.e., it represents the distribution of the noise. It is given, in the case of uncorrelated Gaussian noise with variance σ^2, by:

$$\mathrm{p}(f|g) = \exp\left(-\sum_{pixels} \frac{(f-g)^2}{2\sigma^2}\right) \tag{4}$$

The denominator in Equation (3) is independent of g and is considered as a constant (stationary noise). $\mathrm{p}(g)$ is the a priori distribution of the solution g. In the absence of any information on the solution g except its positivity, a possible course of action is to derive the probability of g from its entropy, which is defined from information theory.

If we know the entropy H of the solution (we describe below different ways to calculate it), we derive its probability by:

$$\mathrm{p}(g) = \exp(-\alpha H(g)) \tag{5}$$

Given the data, the most probable image is obtained by maximizing $\mathrm{p}(g|f)$. This leads to algorithms for noise filtering and to deconvolution [16].

We need a probability density $p(g)$ of the data. The Shannon entropy, H_S [21], is the summing of the following for each pixel,

$$H_S(g) = -\sum_{k=1}^{N_b} p_k \log p_k \tag{6}$$

where $X = \{g_1, ..g_n\}$ is an image containing integer values, N_b is the number of possible values of a given pixel g_k (256 for an 8-bit image), and the p_k values are derived from the histogram of g as $p_k = \frac{m_k}{n}$, where m_k is the number of occurrences in the histogram's kth bin.

The trouble with this approach is that, because the number of occurrences is finite, the estimate p_k will be in error by an amount proportional to $m_k^{-\frac{1}{2}}$ [22]. The error becomes significant when m_k is small. Furthermore this kind of entropy definition is not easy to use for signal restoration, because its gradient is not easy to compute. For these reasons, other entropy functions are generally used, including:

- Burg [23]:

$$H_B(g) = -\sum_{k=1}^{n} \ln(g_k) \tag{7}$$

- Frieden [24]:

$$H_F(g) = -\sum_{k=1}^{n} g_k \ln(g_k) \tag{8}$$

- Gull and Skilling [25]:

$$H_G(g) = \sum_{k=1}^{n} g_k - M_k - g_k \ln\left(\frac{g_k}{M_k}\right) \tag{9}$$

  where M is a given model, usually taken as a flat image

In all definitions n is the number of pixels, and k represents an index pixel. For the three entropies above, unlike Shannon's entropy, a signal has maximum information value when it is flat. The sign has been inverted (see Equation (5)), to arrange for the best solution to be the smoothest.

Now consider the entropy of a signal as the sum of the information at each scale of its wavelet transform, and the information of a wavelet coefficient is related to the probability of it being due to noise. Let us look at how this definition holds up in practice. Denoting h the information relative to a single wavelet coefficient, we define:

$$H(X) = \sum_{j=1}^{l} \sum_{k=1}^{n_j} h(w_{j,k}) \tag{10}$$

with the information of a wavelet coefficient, $h(w_{j,k}) = -\ln p(w_{j,k})$, (Burg's definition rather than Shannon's). l is the number of scales, and n_j is the number of samples in wavelet band (scale) j. For Gaussian noise, and recalling that wavelet coefficients at a given resolution scale are of zero mean, we get

$$h(w_{j,k}) = \frac{w_{j,k}^2}{2\sigma_j^2} + \text{constant} \tag{11}$$

where σ_j is the noise at scale j. When we use the information in a functional to be minimized (for filtering, deconvolution, thresholding, etc.), the constant term has no effect and we can omit it. We see that the information is proportional to the energy of the wavelet coefficients. The larger the value of a normalized wavelet coefficient, then the lower will be its probability of being noise, and the higher will be the information furnished by this wavelet coefficient.

In summary,

- Entropy is closely related to energy, and as shown can be reduced to it, in the Gaussian context.
- Using probability of wavelet coefficients is a very good way of addressing noise, but less good for non-trivial signal.
- Entropy has been extended to take account of resolution scale.

In this section we have been concerned with the following view of the data: $f = g + \alpha + \epsilon$ where observed data f is comprised of original data g, plus (possibly) background α (flat signal, or stationary noise component), plus noise ϵ. The problem of discovering signal from noisy, observed data is important and highly relevant in practice but it has taken us some way from our goal of cluster or segmentation modeling of f – which could well have been cleaned and hence approximate well g prior to our analysis.

An additional reason for discussing the work reported on in this section is the common processing platform provided by entropy.

Often the entropy provides the optimization criterion used (see [13, 16, 26], and many other works besides). In keeping with entropy as having a key role in a common processing platform we instead want to use entropy for cross-model selection. Note that it complements other criteria used, e.g., ML, least squares, etc. We turn now towards a new way to define entropy for application across families of GMM analysis, wavelet transform based approaches, and other approaches besides, all with the aim of furnishing alternative segmentations.

7. Model-Based Rényi Quadratic Entropy

Consider a mixture model:

$$f(x) = \sum_{i=1}^{k} \alpha_i f_i(x) \text{ with } \sum_{i=1}^{k} \alpha_i = 1 \tag{12}$$

Here f could correspond to one level of a mutiple resolution transformed signal. The number of mixture components is k.

Now take f_i as Gaussian:

$$f_i(x) = f_i(x|\mu, V) = \left((2\pi)^{-\frac{m}{2}} |V_i|^{-\frac{1}{2}}\right) \exp\left(-\frac{1}{2}(x-\mu_i)V_i^{-1}(x-\mu_i)^t\right) \tag{13}$$

where $x, \mu_i \in \mathbb{R}^m$, $V_i \in \mathbb{R}^{m \times m}$.

Take

$$V_i = \sigma_i^2 I \tag{14}$$

(I = identity) for simplicity of the basic components used in the model.

A (i) parsimonious (ii) covering of these basic components can use a BIC approximation to the Bayes factor (see section 2) for selection of model, k.

Each of the functions f_i comprising the new basis for the observed density f can be termed a *radial basis* [27]. A radial basis network, in this context, is an iterative EM-like fit optimization algorithm. An alternative view of parsimony is the view of a sparse basis, and model fitting is sparsification. This theme of sparse or compressed sampling is pursued in some depth in [17].

We have:

$$\int_{-\infty}^{\infty} \alpha_i f_i(x|\mu_i, V_i) \, . \, \alpha_j f_j(x|\mu_j, V_j) \, dx \tag{15}$$

$$= \alpha_i \alpha_j f_{ij}(\mu_i - \mu_j, V_i + V_j) \tag{16}$$

See [13] or [26]. Consider the case – apropriate for us – of only distinct clusters so that summing over i, j we get:

$$\sum_i \sum_j (1 - \delta_{ij}) \alpha_i \alpha_j f_{ij}(\mu_i - \mu_j, V_i + V_j) \tag{17}$$

Hence

$$H_{R2} = -\log \int_{-\infty}^{\infty} f(x)^2 \, dx \tag{18}$$

can be written as:

$$-\log \int_{-\infty}^{\infty} \alpha_i f_i(x|\mu_i, V_i) \, . \, \alpha_j f_j(x|\mu_j, V_j) \, dx \tag{19}$$

$$= -\log \sum_i \sum_j (1 - \delta_{ij}) \alpha_i \alpha_j f_{ij}(\mu_i - \mu_j, V_i + V_j) \tag{20}$$

$$= -\log \sum_i \sum_j (1 - \delta_{ij}) f_{ij}(\mu_i - \mu_j, 2\sigma^2 I) \tag{21}$$

from restriction (14) and also restricting the weights, $\alpha_i, \alpha_j = 1, \forall i \neq j$. The term we have obtained expresses interactions beween pairs. Function f_{ij} is a Gaussian. There are evident links here with Parzen kernels [28, 29] and clustering through mode detection (see e.g., [30, 31] and references therein).

For segmentation we will simplify further Equation (20) to take into account just the equiweighted segments reduced to their mean (cf. [28]).

In line with how we defined mutiple resolution entropy in Section 6, we can also define the Rényi quadratic information of wavelet transformed data as follows:

$$H_{R2} = \sum_{s=1}^{S} H_{R2}^s \tag{22}$$

8. Case Study

8.1. Data Analysis System

In this work, we have used MRI (magnetic resonance imaging) and PET (positron emission tomography) image data volumes, and (in a separate study) a data volume of galaxy positions derived from 3D cosmology data. A 3D starlet or B_3 spline à trous wavelet transform is used with these 3D data volumes. Figures 4 and 5 illustrate the system that we built. For 3D data volumes, we support the following formats: FITS, ANALYZE (.img, .hdr), coordinate data (x, y, z), and DICOM; together with AVI video format. For segmentation, we cater for marginal Gaussian mixture modeling, of a 3D image volume. For multivalued 3D image volumes (hence 4D hypervolumes) we used Gaussian mixture modeling restricted to identity variances, and zero covariances, i.e. k-means. Based on a marginal Gaussian mixture model, BIC is used. Rényi quadratic entropy is also supported. A wide range of options are available for presentation and display (traversing frames, saving to video, vantage point XY or YZ or XZ, zooming up to 800%, histogram equalization by frame or image volume). The software, MR3D version 2, is available for download at www.multiresolution.tv. The wavelet functionality requires a license to be activated, and currently the code has been written for PCs running Microsoft Windows only.

Figure 4. Frame number 15 from an MRI brain image.

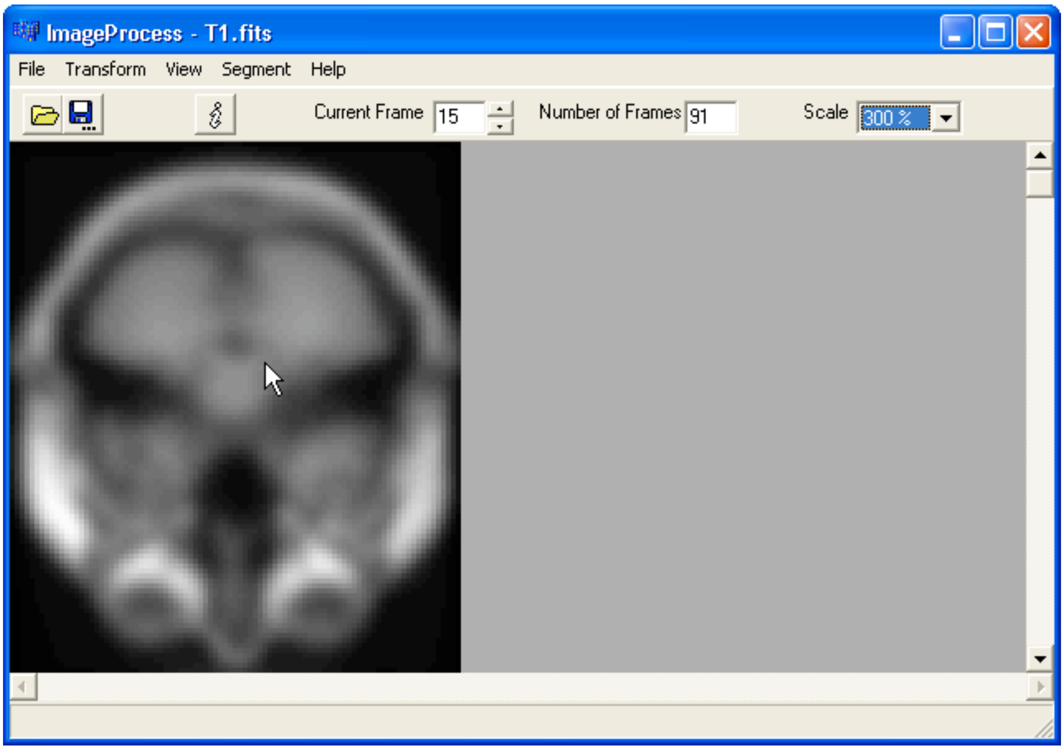

8.2. Segmentation Algorithms Used

Consider T1, an aggregated representative brain, derived from MRI data. It is of dimensions $91 \times 109 \times 91$. See Figure 4. In the work described here as image format for the 3D or 4D image volumes we used the FITS, Flexible Image Transport System, format.

The first model-based segmentation was carried out as follows.

- We use "Marginal Range" in the "Segmentation" pull-down menu to decide, from the plot produced, that the BIC criterion suggests that a 6 cluster solution is best.
- Then we use "Marginal" with 6 clusters requested, again in the "Segmentation" pull-down menu. Save the output as: T1_segm_marg6.fits.

Figure 5. Segmented frame number 15 from an MRI brain image.

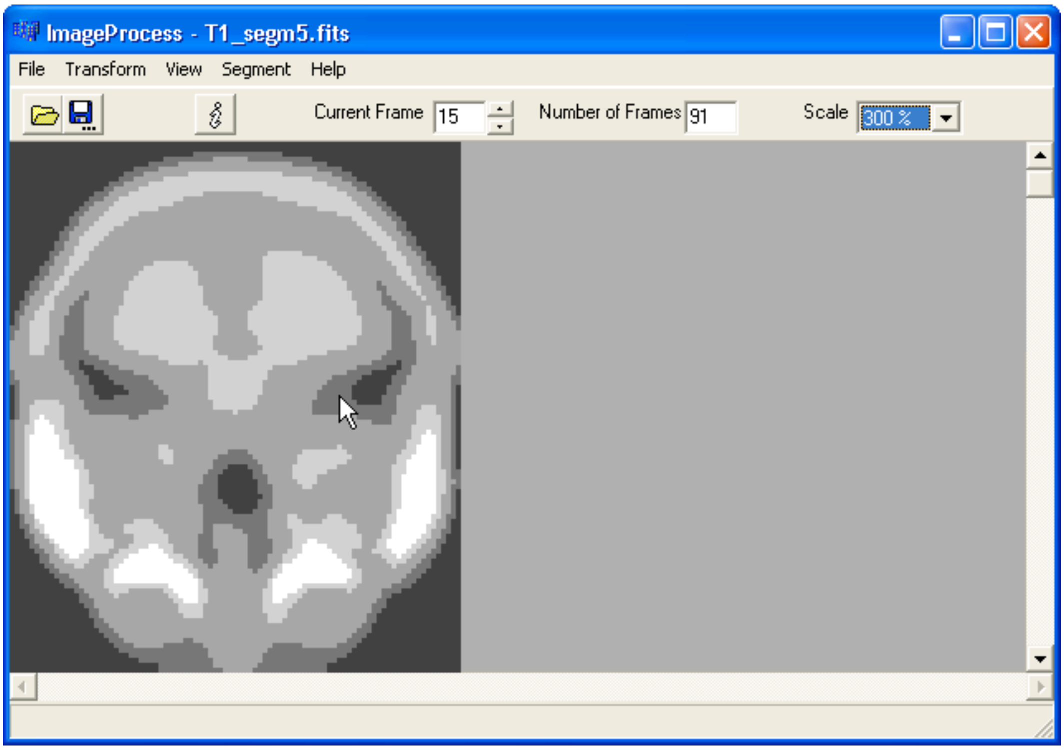

Next an alternative model-based segmentation is carried out in wavelet space.

- Investigate segmentation in wavelet space. First carry out a wavelet transform. The B_3 spline à trous wavelet transform is used with 4 levels (i.e. 3 wavelet resolution scales). The output produced is in files: T1_1.fits, T1_2.fits, T1_3.fits, T1_4.fits.

- Use the wavelet resolution scales as input to "K-Means", in the "Segmentation" pull-down menu. Specify 6 clusters. We used 6 clusters because of the evidence suggested by BIC in the former modeling, and hence for comparability between the two modelings. Save the output as: T1_segm_kmean6.fits.

8.3. *Evaluation of Two Segmentations*

We have two segmentations. The first is a segmentation found from the voxel's marginal distribution function. The second outcome is a segmentation found from the multivalued 3D (hence 4D) wavelet transform.

Now we will assess T1_segm_marg6 versus T1_segm_kmean6. If we use BIC, using the T1 image and first one and then the second of these segmented images, we find essentially the same BIC value. (The BIC values of the two segmentations differ in about the 12th decimal place.) Note though that the model used by BIC is the same as that used for the marginal segmentation; but it is not the same as that used for k-means. Therefore it is not fair to use BIC to assess across models, as opposed to its use within a family of the same model.

Using Rényi quadratic entropy, in the "Segmentation" pull-down menu, we find 4.4671 for the marginal result, and 1.7559 for the k-means result.

Given that parsimony is associated with small entropy here, this result points to the benefits of segmentation in the wavelet domain, i.e. the second of our two modeling outcomes.

9. Conclusions

We have shown that Rényi quadratic entropy provides an effective way to compare model families. It bypasses the limits of intra-family comparison, such as is offered by BIC.

We have offered some preliminary experimental evidence too that direct unsupervised classification in wavelet transform space can be more effective than model-based clustering of derived data. Intended by the latter ("derived data") are marginal distributions.

Our innovative results are very efficient from computational and storage viewpoints. The wavelet transform for a fixed number of resolution scales is computationally linear in the cardinality of the input voxel set. The pairwise interaction terms feeding the Rényi quadratic entropy are also efficient. For both of these aspects of our work, iterative or other optimization is not called for.

Acknowledgements

Dimitrios Zervas wrote the graphical user interface and contributed to other parts of the software described in Section 8.

References

1. McCullagh, P. What is a statistical model? *Ann. Statist.* **2002**, *30*, 1225–1310.
2. Djorgovski, S.G.; Mahabal, A.; Brunner, R.; Williams, R.; Granat, R.; Curkendall, D.; Jacob, J.; Stolorz, P. Exploration of parameter spaces in a Virtual Observatory. *Astronomical Data Analysis* **2001**, *4477*, 43–52.
3. Silk, J. An astronomer's perspective on SCMA III. In *Statistical Challenges in Modern Astronomy*; Feigelson, E.D., Babu, G.J., Eds.; Springer: Berlin, Germany, 2003; pp. 387–394.
4. Nagy, G. State of the art in pattern recognition. *Proc. IEEE* **1968**, *56*, 836–862.
5. Murtagh, F.; Raftery, A.E.; Starck, J.L. Bayesian inference for multiband image segmentation via model-based cluster trees. *Image Vision Comput.* **2005**, *23*, 587–596.
6. Rissanen, J. *Information and Complexity in Statistical Modeling*; Springer: New York, NY, USA, 2007.
7. Hansen, M.H.; Bin, Y. Model selection and the principle of minimum description length. *J. Amer. Statist. Assn.* **2001**, *96*, 746–774.
8. Fraley, C.; Raftery, A.E. How many clusters? Which clustering method? – answers via model-based cluster analysis. *Comput. J.* **1998**, *41*, 578–588.
9. Blum, R.S.; Zhang, Y.; Sadler, B.M.; Kozick, R.J. On the approximation of correlated non-Gaussian noise PDFs using Gaussian mixture models; *Conference on the Applications of Heavy Tailed Distributions in Economics, Engineering and Statistics*; American University: Washington, DC, USA, 1999.

10. Wang, S.; Zhao, Y. Online Bayesian tree-structured transformation of HMMs with optimal model selection for speaker adaptation. *IEEE Trans. Speech Audio Proc.* **2001**, *9*, 663–677.
11. Murtagh, F.; Starck, J.L. Quantization from Bayes factors with application to multilevel thresholding. *Pattern Recognition Lett.* **2003**, *24*, 2001–2007.
12. Murtagh, F.; Starck, J.L. Bayes factors for edge detection from wavelet product spaces. *Opt. Eng.* **2003**, *42*, 1375–1382.
13. Principe, J.C.; Xu, D.X. Information-theoretic learning using Rényi's quadratic entropy; *International Conference on ICA and Signal Separation*; Aussios, France, August 1999; pp. 245–250.
14. Esteban, M.D.; Morales, D. A summary of entropy statistics. *Kybernetika* **1995**, *31*, 337–346.
15. Cachin, C. Entropy Measures and Unconditional Security in Cryptography, Ph.D. Thesis, ETH Zurich: Zurich, Switzerland, 1997.
16. Starck, J.L.; Murtagh, F. *Astronomical Image and Data Analysis*; Springer: Berlin, Germany, 2002. 2nd ed., 2006.
17. Starck, J.L.; Murtagh, F.; Fadili, J. *Sparse Image and Signal Processing: Wavelets, Curvelets, Morphological Diversity*; Cambridge University Press: Cambridge, UK (forthcoming).
18. Murtagh, F.; Starck, J.L.; Berry, M. Overcoming the curse of dimensionality in clustering by means of the wavelet transform. *Comput. J.* **2000**, *43*, 107–120.
19. Murtagh, F.; Starck, J.L. Pattern clustering based on noise modeling in wavelet space. *Pattern Recognition Lett.* **1998**, *31*, 847–855.
20. Starck, J.L.; Murtagh, F.; Gastaud, R. A new entropy measure based on the wavelet transform and noise modeling. *IEEE Transactions on Circuits and Systems – II: Analog and Digital Signal Processing* **1998**, *45*, 1118–1124.
21. Shannon, C.E. A mathematical theory for communication. *Bell Systems Technical Journal* **1948**, *27*, 379–423.
22. Frieden, B. *Probability, Statistical Optics, and Data Testing: A Problem Solving Approach*; 2nd ed.; Springer-Verlag: New York, NY, USA, 1991.
23. Burg, J. Multichannel maximum entropy spectral analysis, Multichannel Maximum Entropy Spectral Analysis; *Annual Meeting International Society Exploratory Geophysics, reprinted in Modern Spectral Analysis*; Childers, D.G., Ed.; IEEE Press: Piscataway, NJ, USA, 1978; pp. 34–41.
24. Frieden, B. Image enhancement and restoration; In *Topics in Applied Physics*; Springer-Verlag: Berlin, Germany, 1975; Vol. 6, pp. 177–249.
25. Gull, S.; Skilling, J. *MEMSYS5 Quantified Maximum Entropy User's Manual*; Maximum Entropy Data Consultants: Cambridge, UK, 1991.
26. Gokcay, E.; Principe, J.C. Information theoretic clustering. *IEEE Trans. Patt. Anal. Mach. Int.* **2002**, *24*, 158–171.
27. MacKay, D.J.C. *Information Theory, Inference, and Learning Theory*; Cambridge University Press: Cambridge, UK, 2003.
28. Lee, Y.J.; Choi, S.J. Minimum entropy, k-means, spectral clustering, In *Proceedings of the International Joint Conference on Neural Networks (IJCNN)*; Budapest, Hungary, July 25–29,

2004; pp. 117–122.

29. Jenssen, R. Information theoretic learning and kernel methods; In *Information Theory and Statistical Learning*; Emmert-Streib, F., Dehmer, M., Eds.; Springer: New York, NY, USA, 2009.
30. Katz, J.O.; Rohlf, F.J. Function-point cluster analysis. *Syst. Zool.* **1973**, *22*, 295–301.
31. Murtagh, F. A survey of algorithms for contiguity-constrained clustering and related problems. *Comput. J.* **1985**, *28*, 82–88.